Rice yield forecasting models using satellite imagery

Research · April 2015

DOI: 10.13140/RG.2.1.2888.3369

CITATIONS
0

READS
151

2 authors, including:

Abdelraouf M Ali
National Authority for Remote Sensing and Space Sciences
22 PUBLICATIONS **99** CITATIONS

SEE PROFILE

The Egyptian Journal of Remote Sensing and Space Sciences (2013) **16**, 125–131

National Authority for Remote Sensing and Space Sciences

The Egyptian Journal of Remote Sensing and Space Sciences

www.elsevier.com/locate/ejrs
www.sciencedirect.com

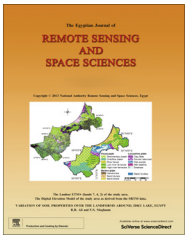

RESEARCH PAPER

Rice yield forecasting models using satellite imagery in Egypt

N.A. Noureldin [a], M.A. Aboelghar [b,*], H.S. Saudy [a], A.M. Ali [b]

[a] *Faculty of Agriculture, Ain Shams University, Egypt*
[b] *National Authority for Remote Sensing and Space Sciences (NARSS), 23, Josef proztito St. Elnozha Elgedida, P.O. Box 1564 Alf maskan, Cairo, Egypt*

Received 7 November 2012; revised 7 April 2013; accepted 22 April 2013
Available online 18 May 2013

KEYWORDS

Vegetation indices;
Leaf area index;
Rice yield prediction

Abstract Ability to make yield prediction before harvest using satellite remote sensing is important in many aspects of agricultural decision-making. In this study, canopy reflectance band and different band ratios in form of vegetation indices (VI) with leaf area index (LAI) were used to generate remotely sensed pre-harvest empirical rice yield prediction models. LAI measurements, spectral data derived from two SPOT data acquired on August 24, 2008 and August 23, 2009 and observed rice yield were used as main inputs for rice yield modeling. Each remotely sensed factor was used separately and in combination with LAI to generate the models. The results showed that green spectral band, middle infra-red spectral band and green vegetation index (GVI) did not show sufficient capability as rice yield estimators while other inputs such as red spectral band, near infrared spectral band and vegetation indices that are algebraic ratios from these two spectral bands when used separately or in combined with leaf area index (LAI) produced high accurate rice yield estimation models. The validation process was carried out using two statistical tests; standard error of estimate and the correlation coefficient between modeled and predicted yield. The validation results indicated that using normalized difference vegetation index (NDVI) combined with leaf area index (LAI) produced the model with highest accuracy and stability during the two rice seasons. The generated models are applicable 90 days after planting in any similar environmental conditions and agricultural practices.

1. Introduction

Crop yield forecasts a few months before harvest can be of paramount importance for timely initiating food trade secure the national demand and timely organize food transport within countries (Bastiaanssen and Ali, 2003). Forecasting enables planners and decision makers to determine how much to import (in shortfall case) or optionally, to export (in surplus

* Corresponding author. Tel.: +20 10 0405188.
E-mail address: mohamed.aboelghar@gmail.com (M.A. Aboelghar).
Peer review under responsibility of National Authority for Remote Sensing and Space Sciences.

Production and hosting by Elsevier

1110-9823 © 2013 Production and hosting by Elsevier B.V. on behalf of National Authority for Remote Sensing and Space Sciences.
http://dx.doi.org/10.1016/j.ejrs.2013.04.005

case). Traditionally, crop yield estimation depended upon data collection technique from ground-based field visits. Such technique is often subjective, costly and is prone to large errors, leading to poor crop assessment and crop area estimation (Reynolds et al., 2000). Also, the obtained data may become available too late for appropriate action to be taken to avert food shortage. At the same time, no yield prediction models unless developed or tested locally are suitable for local use (Shresthan and Naikaset, 2003); this view may be due to soil attributes variation, climatic conditions, plant species varieties and agricultural practices from one area to another. Recently, with successful launching of various satellites, a lot of efforts are made to use remote sensing for yield forecasting. Whereas, remote sensing data have the potential to provide timely, systematically high quality spatial and accurate information about land features including environmental impacts on crop growth (Liu and Kogan, 2002). So, the temporal dynamics of remote sensing data and their close relation with plant characteristics could play a crucial role in establishing an effective pre-harvest yield estimation method.

The most multi spectral satellite systems measure varies spectral bands within the visible to mid-infra red region of the electro magnetic spectrum (Shwetank and Bhatia, 2010). The spectral absorption normally occurs from 670 to 780 nm wave length range of the electro magnetic spectrum (Kempeneers et al., 2004). In this concern, leaf chlorophyll has a strong absorption at 0.45 μm and 0.67 μm, and a high reflectance at near infrared (0.7–0.9 μm). Near infrared is very useful for vegetation surveys and mapping because such a steep gradient at 0.7–0.9 μm is produced only by vegetation (Murai, 1996). Moreover, healthy plants have a high normalized difference vegetation index (NDVI) value because of their high reflectance of infrared light, and relatively low reflectance of red spectrum (Moore and Holden, 2003). The modeling process is based on vegetation indices (VI) which could be observed and collected from remote sensing satellite data as well as remotely sensed ground observation tools. Vegetation indices are optical measures of vegetation canopy "greenness". They give a direct measure of photosynthetic potential resulting from the composite property of total leaf chlorophyll, leaf area, canopy cover, and structure. In this concern, (NDVI) was linked to many plant parameters, which are closely related to crop yield. It has a direct correlation with LAI, biomass and vegetation cover (Wiegand et al., 1990, 1992; Tucker, 1979; Holben et al., 1980; Ahlrichs and Bauer, 1983; Nemani and Running, 1989). These driving parameters are largely influenced by variations in soil fertility (Hinzman and Bauer, 1986) soil moisture (Daughtry et al., 1980; Tucker et al., 1980; Teng, 1990, planting date (Crist, 1984) and crop density (Aase and Siddoway, 1981). Most studies have observed a correlation between NDVI and green biomass yield, therefore NDVI can be used to estimate yield before harvesting (Rasmussen, 1997). The other key for the proposed modeling process is leaf area index (LAI) as a biophysical and major parameter for determining crop growth. It gives a measure of the density of foliage and is closely linked to the photosynthetic and evapotranspiration capacities of plants. It can be regarded as the principle morphological parameter of the vegetation canopy linking the satellite-derived vegetation index and photosynthesis (Bach, 1998). Moreover, VI and LAI have a strong correlation with plant physiological conditions and crop productivity under a different dimension and growth stage with multi-source remote sensing data.

2. Materials and methods

2.1. Field experiment

Yield prediction modeling of rice crop was carried out using the collected data from Sakha experiment station, Agriculture Researcher Center, Ministry of Agriculture, Egypt. The experimental field was situated in the rice belt region which includes Kafr El-Sheikh Governorate. It is located between 31° 06′ 40″ and 31° 06′ 0″ North and 30° 54′ 30″ and 30° 55′ 60″ East (Fig. 1). The total area of rice observation site was 2.4 ha during the growing seasons of 2008 and 2009, cultivated by the variety Sakha 104. The region that includes the study area is defined as Pro-Deltaic Alluvial Plain. This Pro-Delta is characterized by clayey soil of high clay fraction and high water saturation percentages. These clayey soils are characterized as Vertisols of Typic Haplotonerts, fine, and thermic (Afify et al., 2011). Rice was sown in May 24th and 23rd in the 1st and 2nd seasons, respectively. At 90 days from sowing (maximum vegetative growth stage), sixty measurements were collected from sixty parcels of the rice field in each season based on the grid system (Fig. 2). Each parcel covers 400 m^2 (20 × 20 m) that represents a single SPOT pixel that was fixed as one plot of measurements. The location of the center square meter of each plot was recorded using global positioning system (GPS). Out of this number, fifty random samples were selected for the modeling process and ten samples were selected for validation. Three types of data were used as inputs for generating rice yield prediction models: the direct spectral data collected from SPOT imagery (reflectance values of green, red and near infrared bands), six calculated vegetation indices values, as well as the values of observed rice yield and LAI.

2.2. Satellite data

Four spectral reflectance data were released from the different SPOT bands: green (0.50–0.59 lm), red (0.61–0.68 lm), near infrared (0.78–0.89 lm) and middle infrared (1.58–1.75 lm) acquired during the rice seasons in August of 2008 and 2009. In this respect, two satellite imageries of SPOT4 were acquired to cover rice field within the same indexed projection of K111/J287 including multispectral data. The acquisition dates of these images were in August 24, 2008 and August 23, 2009. The images were geometrically, radiometrically and atmospherically corrected. FLAASH model under ENVI software was used for atmospheric correction. It provides accurate, physics-based derivation of apparent surface reflectance through derivation of atmospheric properties such as surface albedo, surface altitude, water vapor column, aerosol and cloud optical depths, surface and atmospheric temperatures from HSI data. FLAASH operates in the 0.4–2.5 μm spectral range. First, MODTRAN simulations of spectral radiance are performed for various atmospheric, water vapor, and viewing conditions (solar angles) over a range of surface reflectance to establish lookup tables for the atmospheric parameters of column water vapor, aerosol type, and visibility for subsequent

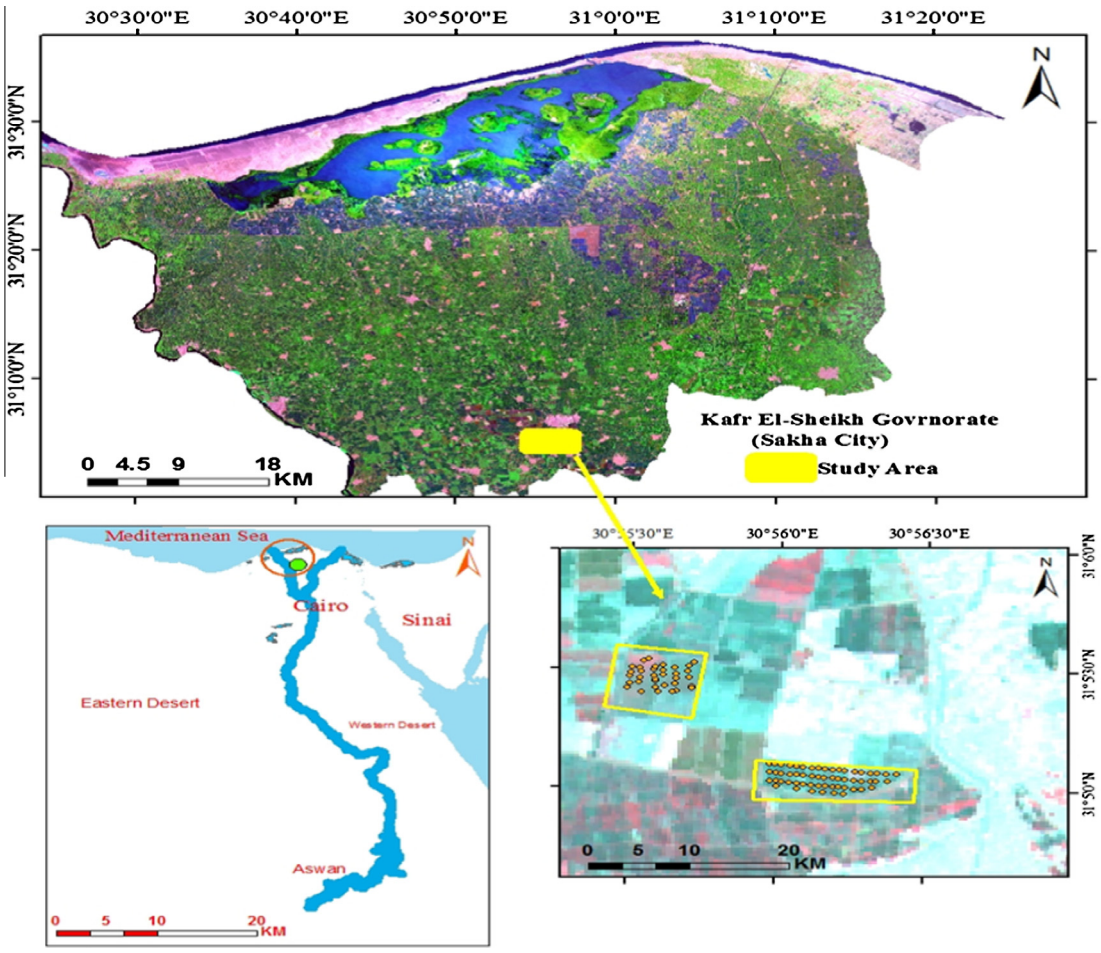

Figure 1 Field experiment location.

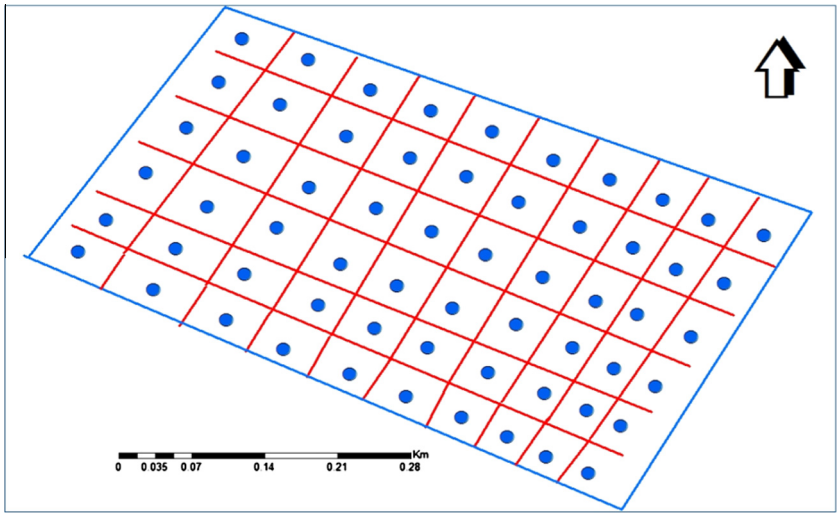

Figure 2 Cell grid system for collecting samples in rice field.

use. Typically, the 1.13 μm water band is used to estimate water vapor, and a ratio of in-band and out-of-band radiance values allows estimation of absorption band depths for a range of water vapor column densities. FLAASH also derives pressure altitudes by applying the same method to the oxygen 0.762 μm absorption band. FLAASH offers the additional option of correcting for light scattered from adjacent pixels. Spatially averaged reflectance is used to account for the

"adjacency effect" – radiance contributions that, because of atmospheric scattering, originate from parts of the surface not in the direct line of sight of the sensor (Adler-Golden et al., 1999; Matthew et al., 2003). The SPOT image was calibrated by resembling the original image based on the mathematical model to leave the image's spectral information undisturbed.

2.3. Vegetation indices (VI)

Five vegetation indices were calculated from different forms of algebraic ratios between red (R) and near-infrared bands: (NIR) Ratio Vegetation Index (RVI), Infrared Percentage Vegetation Index (IPVI), Difference Vegetation Index (DVI), Normalized Difference Vegetation Index (NDVI) and Soil Adjusted Vegetation Index (SAVI), in addition to one vegetation index was calculated through a ratio between green band and near-infrared band: Green Vegetation Index (GVI). All vegetation indices were calculated from SPOT 4 data. These vegetation indices were calculated as follows:

1- GVI (Panda et al., 2010):

$$\mathrm{GVI} = \frac{\rho_{\mathrm{ir}} - \rho_{\mathrm{g}}}{\rho_{\mathrm{ir}} + \rho_{\mathrm{g}}}$$

where: ρ_{ir} and ρ_{g} are spectral reflectance from the green and NIR band images, respectively.

2- RVI (Jordan, 1969):

$$\mathrm{RVI} = \frac{\mathrm{NIR}}{\mathrm{Red}}$$

3- IPVI (Crippen, 1990):

$$\mathrm{IPVI} = \frac{\mathrm{NIR}}{\mathrm{NIR} + \mathrm{R}}$$

It is restricted to values between 0 and 1 and eliminates the conceptual strangeness of negative values for vegetation indices.4- DVI (Richardson and Everitt, 1992):

$$\mathrm{DVI} = \mathrm{NIR} - \mathrm{Red}$$

5- NDVI (Rouse et al., 1973):

$$\mathrm{NKVI} = \frac{\rho_{\mathrm{ir}} - \rho_{\mathrm{r}}}{\rho_{\mathrm{ir}} + \rho_{\mathrm{r}}}$$

where: ρ_{r} and ρ_{ir} are spectral reflectance from the R and NIR band images, respectively.6- SAVI

$$\mathrm{SAVI} = \left[\frac{\rho_{\mathrm{ir}} - \rho_{\mathrm{r}}}{\rho_{\mathrm{ir}} + \rho_{\mathrm{r}} + L}\right] \cdot (1 + L)$$

where ρ_{r} and ρ_{ir} are spectral reflectance from the R and NIR band images, respectively, and L is an optimal adjustment factor. Huete (1988) defined the optimal adjustment factor of $L = 0.25$, 0.5 or 1.0 to be considered for higher, intermediate or low vegetation density in the field, respectively. He suggested that SAVI ($L = 0.5$) successfully minimized the effect of soil variations in green vegetation compared to NDVI. Based on our observations, we considered canopy cover of the rice crop in the field as intermediately dense during the time of satellite images acquisition in 2008 and 2009. Thus, the value of 0.5 was used as the L factor using the Huete strategy of selecting the L factor, which is also supported by Thiam and Eastmen (1999).

2.4. Leaf area index (LAI)

Leaf area index (LAI) and actual rice yield were measured. In this concern, within each parcel, five LAI readings were collected using LAI-2000 plant canopy analyzer, and then the average was recorded. At the end of each rice season, a harvester was used to measure the yield of each parcel and the average yield (ton/ha) was calculated. Finally, the whole dataset was completed as sixty points for each rice season, LAI measurements, and spectral variables including red and near infrared bands represented as digital numbers and six vegetation indices. All generated models are site specific limited to the area and the surrounding environment and could be applicable under similar conditions in Egypt.

The separate bands and separate VI images of the test site were transformed into ASCII format and MS-Excel macro program is written to collect reflectance of all values. All vegetation indices values and LAI are considered for the regression analysis and integrated yield prediction models of the two rice seasons. The explanatory power of the independent variables in the model and eventual prediction accuracy of the generated models were assessed with statistical parameters i.e., standard error of estimate (SEE) and determination coefficient (R^2).The generated models were validated through two main steps: The first step is the determination coefficient that is released from the generated models while the second step is the validation of the models through testing the yield that is calculated through the generated models (modeled yield) against the yield that is observed from the technical office of Sakha Experimental Station (observed yield). Testing modeled yield against observed yield was carried out through two common statistical tests i.e., the standard error of estimate between modeled yield and observed yield as well as the determination coefficient for a direct regression analysis between modeled and observed yield for each generated model.

3. Results and discussion

3.1. Regression analysis

3.1.1. Simple regression analysis

Through studying the simple regression relationships and computing coefficients of determination (R^2) between rice yield, as a dependent variable, and each of green band, red band, NIR band, MIDIR band, GVI, DVI, IPVI, RVI, NDVI, SAVI and LAI as independent ones, it is shown that the suitable mathematical uniform is the linear one (Table 1).

According to regression equations, there is a distinctive relation between rice yield either with red band, NIR band, DVI, IPVI, RVI, NDVI, SAVI and LAI, while, green band, mid-infrared and GVI models showed the lowest determination coefficient. From R^2 value, of each, it is observed that 83–75%, 86–84%, 88–85%, 85–80%, 89–86%, 85–80%, 85–80% and 83–81% of the changes in rice yield were attributed to red band, NIR band, DVI, IPVI, RVI, NDVI, SAVI and LAI, in 2008 and 2009 seasons respectively. Additionally, regression equations predict that the more the NIR band, DVI, IPVI, RVI, NDVI, SAVI and LAI increase as well as red band decreases by one unit, the more the rice yield increases by 0.11, 47.1, 2.52, 23.5, 18.8, 2.87 and 0.92 ton/ha., respectively as averages of the two studied seasons. The valida-

Table 1 Simple regression models for rice yield prediction in 2008 and 2009 seasons.

Forecaster	2008 Season		2009 Season	
	Model	R^2	Model	R^2
Green band	$Y = 3.474 + 0.159 \times \text{Green}$	0.11	$Y = 6.106 + 0.097 \times \text{Green}$	0.04
Red band	$Y = 35.969–0.932 \times \text{Red}$	0.83	$Y = 35.400–0.913 \times \text{Red}$	0.75
NIR band	$Y = -2.516 + 0.130 \times \text{IR}$	0.86	$Y = -2.162 + 0.127 \times \text{IR}$	0.84
MIDIR band	$Y = 3.481 + 0.161 \times \text{MIDIR}$	0.24	$Y = 3.869 + 0.154 \times \text{MIDIR}$	0.27
GVI	$Y = 4.554 + 13.954 \times \text{GVI}$	0.31	$Y = 4.818 + 13.367 \times \text{GVI}$	0.33
DVI	$Y = 1.988 + 0.117 \times \text{DVI}$	0.88	$Y = 2.233 + 0.115 \times \text{DVI}$	0.85
IPVI	$Y = -27.165 + 48.323 \times \text{IPVI}$	0.85	$Y = -25.283 + 45.857 \times \text{IPVI}$	0.80
RVI	$Y = 1.039 + 2.537 \times \text{RVI}$	0.89	$Y = 1.237 + 2.504 \times \text{RVI}$	0.86
NDVI	$Y = -.003 + 24.161 \times \text{NDVI}$	0.85	$Y = -2.355 + 22.928 \times \text{NDVI}$	0.80
SAVI	$Y = -2.987 + 19.343 \times \text{SAVI}$	0.85	$Y = -2.34 + 18.357 \times \text{SAVI}$	0.80
LAI	$Y = -0.386 + 2.753 \times \text{LAI}$	0.83	$Y = -1.357 + 2.995 \times \text{LAI}$	0.81

R^2: Determination coefficient.

Table 2 Determination coefficient (R^2) and standard error of estimation (SEE) of actual and predicted rice yield of different spectral bands obtained from satellite imagery, vegetation indices and LAI in 2008 and 2009 seasons.

Forecaster	2008 Season		2009 Season	
	R^2	SEE	R^2	SEE
Green band	0.05	0.894	0.06	0.545
Red band	0.91	0.716	0.9	0.741
NIR band	0.92	0.727	0.91	0.755
MIDIR band	0.24	1.090	0.24	1.050
GVI	0.40	1.260	0.39	1.220
DVI	0.94	0.641	0.93	0.684
IPVI	0.93	0.706	0.92	0.722
RVI	0.95	0.578	0.94	0.624
NDVI	0.93	0.706	0.92	0.722
SAVI	0.92	0.760	0.92	0.722
LAI	0.85	0.900	0.85	0.989

tion of these models was carried out using two statistical analyses including regression analysis between actual and expected yield for each model and R^2 values as well as the standard error of estimation (SEE) as presented in Table 2. It is observed in the 1st and 2nd seasons that green band, mid-infra-red and GVI as predictors for rice yield prediction models are not applicable as they showed low determination coefficient ($R^2 = 0.4$ in the best case). Contrarily, the other models were adequate for predicting rice yield as they recorded higher than 0.8 of R^2 for each. Such analysis almost agreed with the result of the analysis of the SEE as shown in Table 2.

3.1.2. Multi-regression analysis

Multi-regression analysis and determination coefficient were performed based on the combination between leaf area index (LAI) as a measured biophysical parameter and each of different spectral parameters that was obtained from satellite imagery either in the form of spectral bands or vegetation indices in 2008 and 2009 seasons (Table 3).

Regarding the generated multi-regression formula and the determination coefficient of each generated model, using more than one variable for rice yield prediction increased the efficiency of the accuracy of the generated models due to enhancing R^2 values, except with the case of mid-infra-red model in 2008 season where its R^2 was 0.24. As performed with the case of simple regression, the validation process was performed using regression analysis between actual and predicted yield and calculating R^2 values for the different models as well as the standard error of estimation as shown in Table 4. All models revealed acceptable results and the accuracy of all models was comparable to each other where relatively high values of R^2 and low values of SEE were recorded. However, it is not recommended to use simple regression models based on green and mid-infra-red bands, where they appeared to have low accuracy and multi-regression model of mid-infra-red band where it was not stable through the two studied seasons.

It is clear that the obtained predictors derived from satellite imagery either in the form of spectral bands (red and NIR) or vegetation indices (DV, IPVI and SAVI) are the more effective spectral parameters for forecasting rice yield. These results could be attributed to that red and NIR bands are the most related wavelengths for chlorophyll synthesis or chlorophyll light absorption. In this concern, total chlorophyll content was linearly related to the reflectance in the red-edge (between 700 and 710 nm and NIR (between 750 and 800 nm) ranges using the equation. The results of the generated models also agreed with Gitelson et al., 2003; Bendict and Swindler, 1961; Thomas and Oerther, 1972; Xiao et al., 2005 who found that chlorophyll of green leaves absorbed 80–90% of light in blue (about 0.45 μm) or red portion (about 0.68 μm) of spectrum. The

Table 3 Multi-regression models for rice yield prediction in 2008 and 2009 seasons.

Forecaster	2008 Season		2009 Season	
	Model	R^2	Model	R^2
Green band/LAI	$Y = 4.252 + 3.405 \times \text{LAI} - .172 \times \text{GREEN}$	0.91	$Y = 3.179 + 3.640 \times \text{LAI} - 0.170 \times \text{GREEN}$	0.90
Red band/LAI	$Y = 18.550 + 1.369 \times \text{LAI} - 0.192 \times \text{Red}$	0.85	$Y = 9.383 + 2.184 \times \text{LAI} - 0.276 \times \text{Red}$	0.81
NIR band/LAI	$Y = -2.848 + 1.436 \times \text{LAI} + 0.077 \times \text{IR}$	0.86	$Y = -3.139 + 1.541 \times \text{LAI} + 0.076 \times \text{IR}$	0.91
MIDIR band/LAI	$Y = -.539 + 2.586 \times \text{LAI} + 0.118 \times \text{MIDIR}$	0.24	$Y = -5.309 + 2.794 \times \text{LAI} + 0.117 \times \text{MIDIR}$	0.96
GVI/LAI	$Y = -2.631 + 2.841 \times \text{LAI} + 8.342 \times \text{GVI}$	0.93	$Y = -3.189 + 2.658 \times \text{LAI} + 7.899 \times \text{GVI}$	0.91
DVI/LAI	$Y = 0.092 + 1.310 \times \text{LAI} + 0.073 \times \text{DVI}$	0.88	$Y = -0.260 + 1.445 \times \text{LAI} + 0.070 \times \text{DVI}$	0.91
IPVI/LAI	$Y = -6.889 + 1.418 \times \text{LAI} + 28.003 \times \text{IPVI}$	0.85	$Y = -15.569 + 1.684 \times \text{LAI} + 24.917 \times \text{IPVI}$	0.88
RVI/LAI	$Y = -0.185 + 1.131 \times \text{LAI} + 1.675 \times \text{RVI}$	0.93	$Y = -0.486 + 1.269 \times \text{LAI} + 1.619 \times \text{RVI}$	0.90
NDVI/LAI	$Y = 2.887 + 1.418 \times \text{LAI} + 14.002 \times \text{NDVI}$	0.92	$Y = -3.110 + 1.684 \times \text{LAI} + 12.458 \times \text{NDVI}$	0.88
SAVI/LAI	$Y = -.882 + 1.418^{*}\text{LAI} + 6.6226^{*}\text{SAVI}$	0.92	$Y = -3.102 + 1.684 \times \text{LAI} + 9.979 \times \text{SAVI}$	0.89

R^2: Determination coefficient; SEE: Standard error estimation.

Table 4 Determination coefficient (R^2) and standard error of estimation (SEE) of actual and predicted rice yield of LAI and each of different spectral parameters obtained from satellite imagery either in form of spectral bands or vegetation indices in 2008 and 2009 seasons.

Forecaster	2008 Season		2009 Season	
	R^2	SEE	R^2	SEE
Green band/LAI	0.95	0.581	0.95	0.625
Red band/LAI	0.89	0.559	0.89	0.873
NIR band/LAI	0.97	0.445	0.97	0.462
MIDIR band/LAI	0.96	0.489	0.96	0.518
GVI/LAI	0.96	0.549	0.96	0.514
DVI/LAI	0.97	0.449	0.97	0.466
IPVI/LAI	0.96	0.490	0.96	0.529
RVI/LAI	0.96	0.499	0.96	0.518
NDVI/LAI	0.96	0.490	0.96	0.529
SAVI/LAI	0.96	0.429	0.96	0.529

results agreed also with Rouse et al. (1973) who found that red band (0.63–0.70 μm) and near infrared band (0.75–1.0 μm) were the most suitable portions from the Electro-Magnetic Spectrum (EMS) that could be used for the assessment of crop conditions and biomass as the red spectral interval corresponds to region of maximum chlorophyll absorption while the near infrared spectral interval corresponds to maximum reflectance of incident light by living vegetation. The study also confirmed the importance of LAI as a biophysical trait for determining crop growth being a measure of the density of foliage and is closely linked to the photosynthetic capacities of plants and consequently their productivity. LAI as the principle morphological parameter of the vegetation canopy could be used successfully to link the satellite-derived vegetation index and photosynthesis. It is expected that the generated models are applicable using SPOT data in any area with similar environmental conditions. Applying these models using other types of satellite imagery may not give the same accuracy. The reason of this could be the difference in the spectral band ranges of the other data. This will make a difference in the values of the vegetation indices.

4. Conclusion

In the current study, after observing the results of all generated models for rice yield prediction for the two seasons of 2008 and 2009 and the validation analysis for the generated models, it could be concluded that using multi-regression model of LAI as one input factor and NDVI or any other vegetation index that is calculated from red and near infrared spectral reflectance under normal environmental conditions and common agricultural practices during the period of the maximum vegetative growth could be the best methodology of rice yield forecasting using satellite imagery. Using high resolution satellite imagery is necessary to be able to isolate rice cultivation especially in the intensive agricultural lands of Nile Delta in Egypt and it is also necessary to apply these models over national scale. All generated models are empirical models limited to environmental conditions and applicable under similar conditions.

References

Aase, J.K., Siddoway, F.H., 1981. Spring wheat yield estimates from spectral reflectance measurements. IEEE Transactions on Geoscience and Remote Sensing 19 (2), 78–84.

Adler-Golden, S.M., Matthew, M.W., Bernstein, L.S., Levine, R.Y., Berk, A., Richtsmeier, S.C., Acharya, P.K., Anderson, G.P., Felde, G., Gardner, J., Hike, M., Jeong, L.S., Pukall, B., Mello, J., Ratkowski, A., Burke, H., 1999. Atmospheric correction for shortwave spectral imagery based on MODTRAN4. SPIE Proceedings Imaging Spectrometry 3753, 61–69.

Afify, A.A., Aboelghar, M.A., Arafat, S.M., Afify, N.M., Yonis, M.S., 2011. Delineating rice belt cultivation in the Nile pro-delta of Vertisols using remote sensing data of EgyptSat-1. Minufiya Journal Agriculture Research 35 (6), 2263–2279.

Ahlrichs, J.S., Bauer, M.E., 1983. Relation of agronomic and multispectral reflectance characteristics of spring wheat canopies. Agronomy Journal 75, 987–993.

Bach, H., 1998. Yield estimation of corn based on multitemporal LANDSAT-TM data as input for agrometeorological model. Pure and Applied Optics 7, 809–825.

Bastiaanssen, W.G.M., Ali, S., 2003. A new crop yield forecasting model based on satellite measurements applied across the Indus Basin Pakistan. Agriculture Ecosystem and Environment 94, 321–340.

Bendict, H.M., Swindler, R., 1961. Nondestructive method for estimating chlorophyll content of leaves. Science 1333, 2015–2016.

Wiegand, C.L., Mass, S.J., K Aasse, J., Hartfield, J.L., Pinter, P.J., Jackson, R.D., Kanemasu, E.T., Lapitan, R.L., 1992. Multisite analyses of spectral-biophysical data for wheat. Remote Sensing of Environment 42, 1–21.

Crippen, R.E., 1990. Calculating the vegetation index faster. Remote Sensing of Environment 34, 71–73.

Crist, E.P., 1984. Effects of cultural and environmental factors of corn and soybean spectral development pattern. Remote Sensing of Environment 14, 3–13.

Daughtry, C.S.T., Bauer, M.E., Cresclius, D.W., Hixon, M.M., 1980. Effects of management practices on reflectance of spring wheat canopies. Agronomy Journal 72, 1055–1060.

Gitelson, A.A., Gritz, Y., Merzlyak, M.N., 2003. Relations between leaf chlorophyll content and spectral reflectance and algorithms for non-destructive chlorophyll assessment in higher plant leaves. Journal of Plant Physiology 160, 271–282.

Hinzman, L.D., Bauer, M.E., Daughtry, C.S.T., 1986. Effects of nitrogen fertilization on growth and reflectance characteristics of winter wheat. Remote Sensing of Environment 19, 47–61.

Holben, B.N., Tucker, C.J., Fan, C.J., 1980. Spectral assessment of soybean leaf area and leaf biomass. Photogrammetric Engineering and Remote Sensing 46 (5), 651–656.

Huete, A.R., 1988. Soil adjusted vegetation index (SAVI). Remote Sensing of Environment 25, 295–309.

Jordan, C.F., 1969. Derivation of leaf area index from quality of light on the forest floor. Ecology 50, 663–666.

Kempeneers, P., Backer, D., Debruyn, W., Scheunders, P., 2004. Wavelet based feature extraction for hyper spectral vegetation monitoring, Image and Signal Processing for Remote Sensing IX. Proceedings of the SPIE 5238, 297–305.

Liu, W.T., Kogan, F., 2002. Monitoring Brazilian soybean production using NOAA/AVHRR based vegetation condition indices. International Journal of Remote Sensing 23 (6), 1161–1179.

Moore, J., Holden, N.M., 2003. Examining the development of a potato crop nutrient management trial using reflectance sensing. ASAE Annual International Meeting. Las Vegas, Nevada, USA.

S. Murai (1996). GIS Workbook, from <http://ksrs.or.kr/library/index.htm>.

Nemani, R.R., Running, S.W., 1989. Testing a theoretical climate-soil leaf area hydrological equilibrium of forests using satellite data and ecosystem simulation. Agriculture and Forest Meteorology 44, 245–260.

Panda, S.S., Ames, D.P., Panigrahi, S., 2010. Application of vegetation indices for agricultural crop yield prediction using neural network techniques. Remote Sensing 2, 673–696.

Rasmussen, M.S., 1997. Operational yield forecast using AVHRR NDVI data: reduction of environmental and inter-annual variability. International Journal of Remote Sensing 18 (5), 1059–1077.

Reynolds, C.A., Yitayew, M., Slack, D.C., Hutchinson, C.F., Huete, A., Petersen, M.S., 2000. Estimating crop yields and production by integrating the FAO crop specific water balance model with real-time satellite data and ground-based ancillary data. International Journal of Remote Sensing 21, 3487–3508.

Richardson, A.J., Everitt, J.H., 1992. Using spectra vegetation indices to estimate rangeland productivity. Geocarto International 7 (1), 63–69.

Rouse, J.W., Haas, R.H., Schell, J.A., Deering, D.W., 1973. Monitoring vegetation systems in the great plains with ERTS. 3rd ERTS Symposium, NASA SP-351 1, 309–317.

Shresthan, R.P., Naikaset, S., 2003. Agro-spectral models for estimating dry season rice yield in the Bangkok Plain of Thailand. Asian Journal of Geoinformatics 4, 11–19.

Shwetank, J.K., Bhatia, K.F., 2010. Review of rice crop identification and classification using hyper spectral image processing system. International Journal of Computer Science & Communication 1 (1), 253–258.

Teng, W.L., 1990. AVHRR monitoring of U.S. crops during the (1988) drought. Photogrammetric Engineering and Remote Sensing 56 (8), 1143–1146.

Thiam, S., Eastmen, R.J., 1999. Chapter on vegetation indices. In: Guide to GIS and Image Processing, vol. 2. Idrisi Production, Clarke University, Worcester, MA, USA, pp. 107–122.

Thomas, J.R., Oerther, G.F., 1972. Estimating nitrogen content of sweet pepper leaves by reflectance measurements. Agronomy Journal 64, 11–13.

Tucker, C.J., 1979. Red and photosynthetic infrared linear combination for monitoring vegetation. Remote Sensing of Environment 8, 127–150.

Tucker, C.J., Holben, J.R., McMutrey, J.E., 1980. Relation of spectral data to grain yield variation. Photogram Engineering and Remote Sensing 46, 657–666.

Matthew, M.W., Adler-Golden, S.M., Berk, A., Felde, G., Anderson, G.P., Gorodestzky, D., Paswaters, S., Shippert, M., 2003. Atmospheric correction of spectral imagery: evaluation of the FLAASH algorithm with AVIRIS data. In: SPIE Proceeding, Algorithms and Technologies for Multispectral, Hyperspectral, and Ultraspectral Imagery IX.

Wiegand, C.L., Rechardson, A.J., Escobar, D.E., Gerbermann, A.H., 1990. Vegetation indices in crop assessment. Remote Sensing of Environment 35, 105–119.

Xiao, X.T.S., Boles, J.Y., Liu, D., Zhuang, S., Frolking, S., Li, C., Salas, W., Moore, B., 2005. Mapping paddy rice agriculture in southern China using multi-temporal MODIS images. Remote Sensing of Environment 95, 480–492.